Electronic Supplementary Information for:

Stepwise Photochromism of Bisnaphthopyrans Exhibiting Excitation Intensity-Dependent Color Change

Yuki Inagaki,[†] Katsuya Mutoh[†] and Jiro Abe*, [†]

[†]*Department of Chemistry, School of Science and Engineering, Aoyama Gakuin University, 5–10–1 Fuchinobe, Chuo–ku, Sagamihara, Kanagawa 252–5258, Japan*

E–mail: *jiro abe@chem.aoyama.ac.jp*

CONTENTS

1. NMR Spectra

^{1}H NMR Spectra

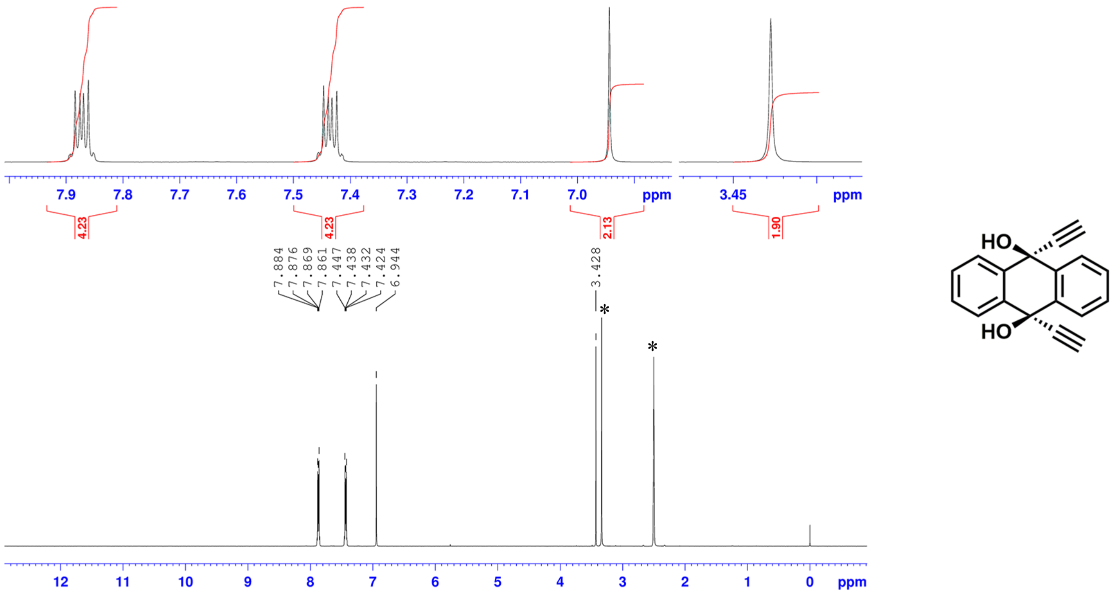

Fig. S1 ^{1}H NMR spectrum of (9s, 10s)-9,10-diethynyl-9,10-dihydroanthracene-9,10-diol in DMSO-d_6 (* solvent peaks).

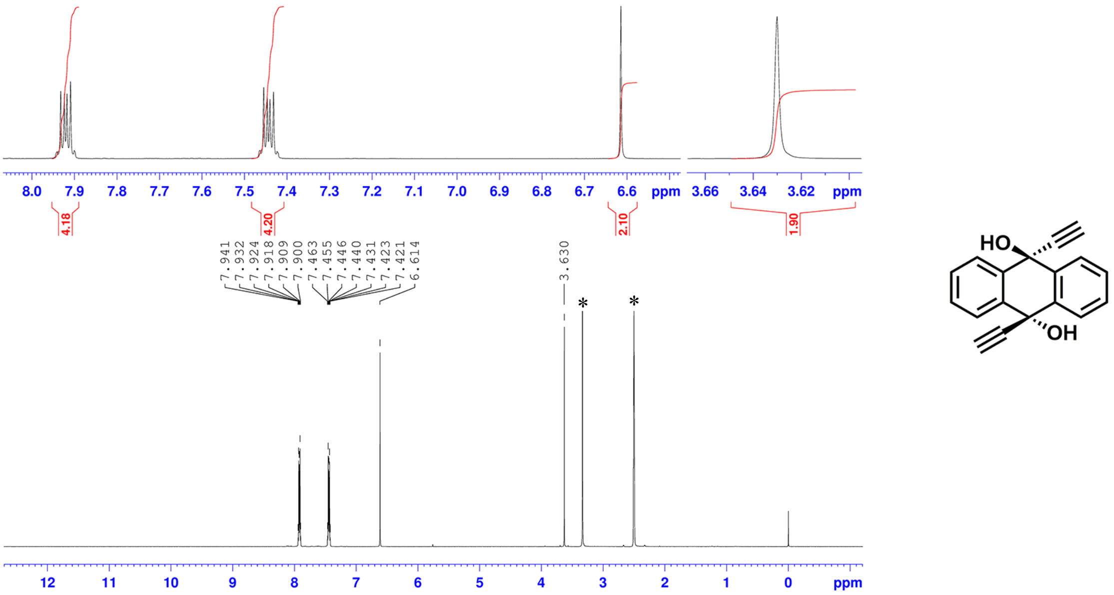

Fig. S2 ^{1}H NMR spectrum of (9*r*, 10*r*)-9,10-diethynyl-9,10-dihydroanthracene-9,10-diol in DMSO-d_6 (* solvent peaks).

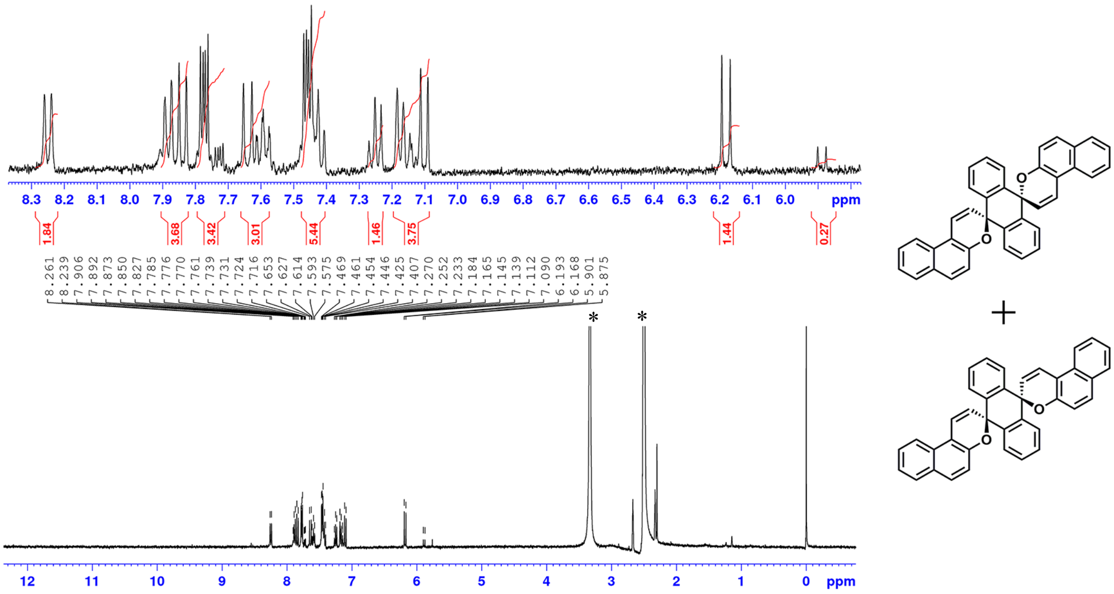

Fig. S3 ^{1}H NMR spectrum of **bis-NP** in DMSO-d_6 (* solvent peaks).

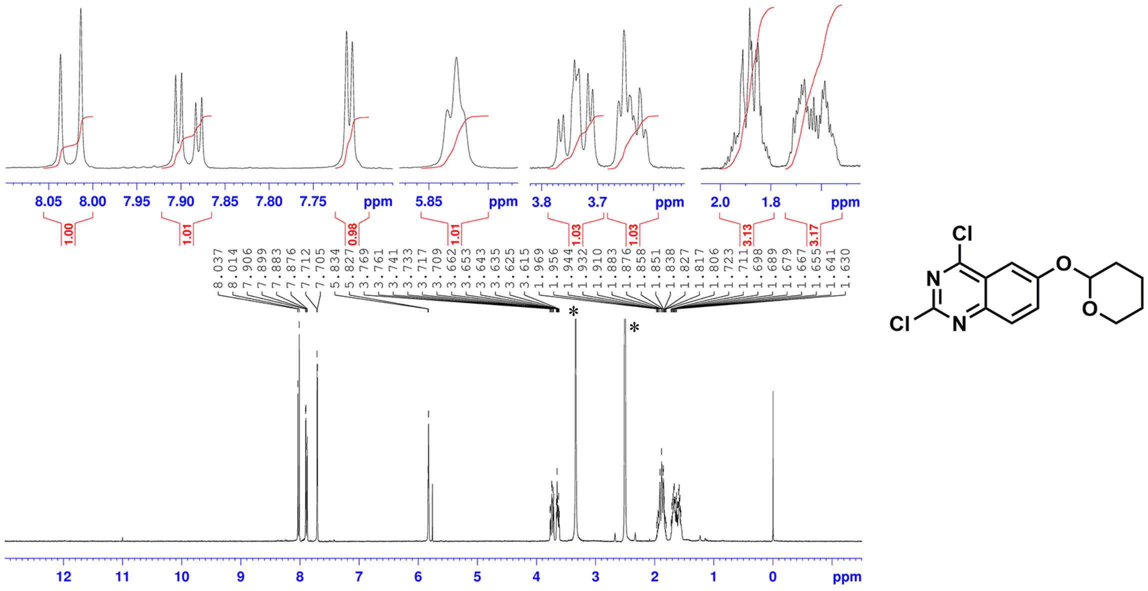

Fig. S4 ^{1}H NMR spectrum of 2,4-dichloro-6-((tetrahydro-2*H*-pyran-2-yl)oxy)quinazoline in DMSO-d_6 (* solvent peaks).

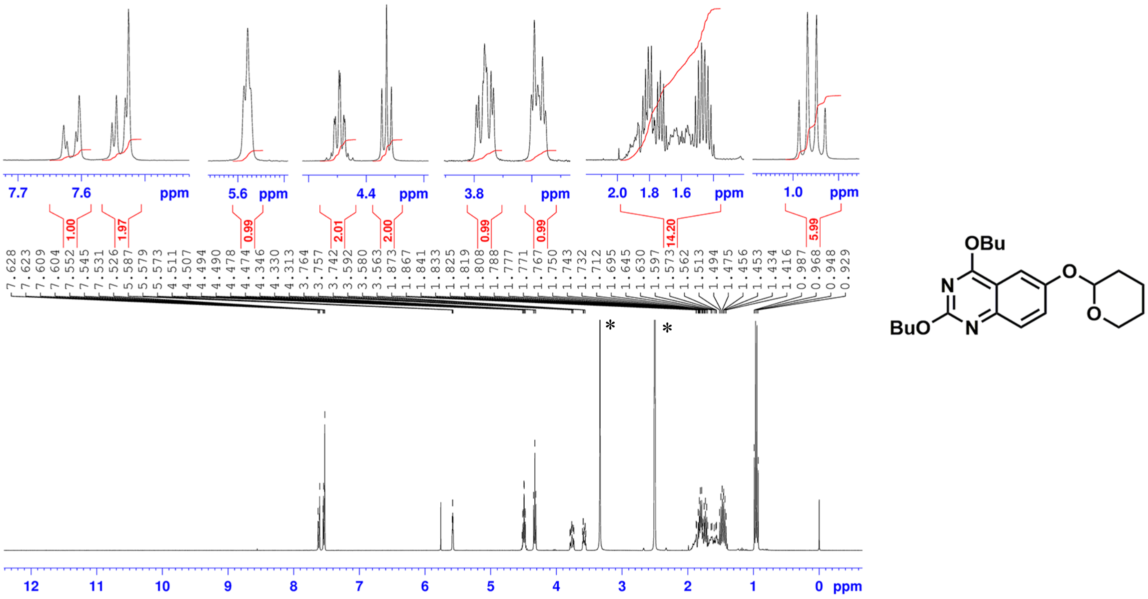

Fig. S5 ^{1}H NMR spectrum of 2,4-dibutoxy-6-((tetrahydro-2*H*-pyran-2-yl)oxy)quinazoline in DMSO-d_6 (* solvent peaks).

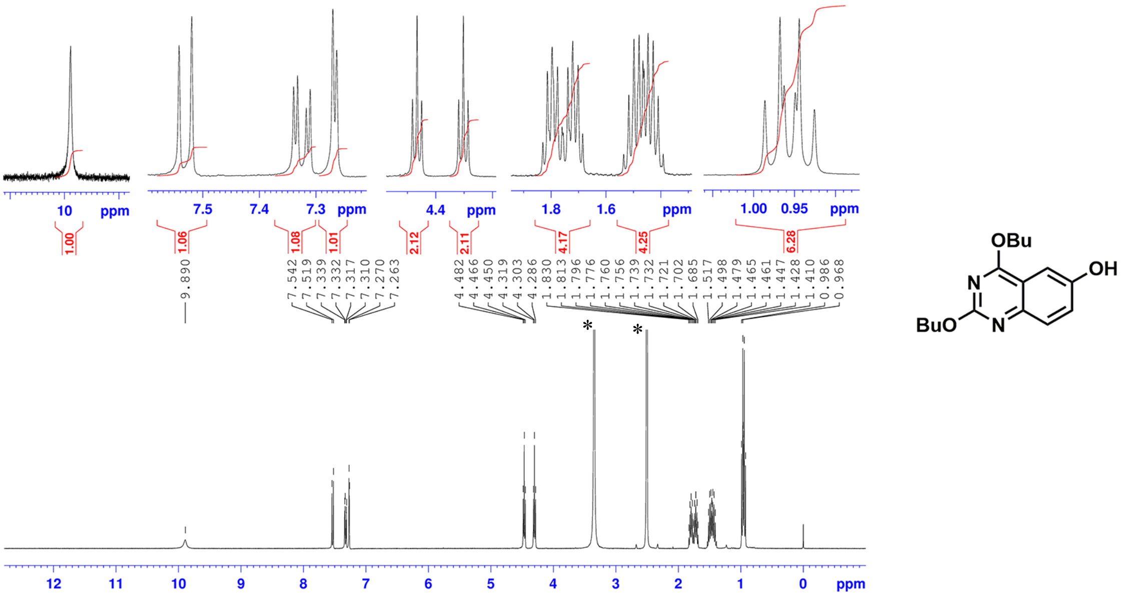

Fig. S6 ^{1}H NMR spectrum of 2,4-dibutoxyquinazolin-6-ol in DMSO-d_6 (* solvent peaks).

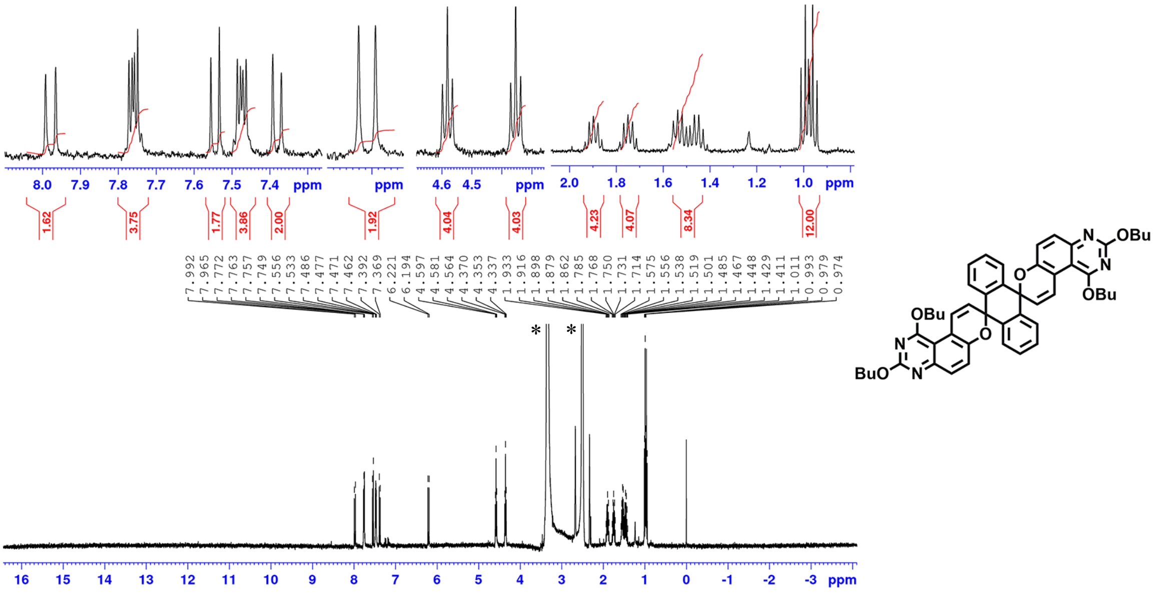

Fig. S7 ^{1}H NMR spectrum of **bis-PQ** in DMSO-d_6 (* solvent peaks).

^{13}C NMR Spectra

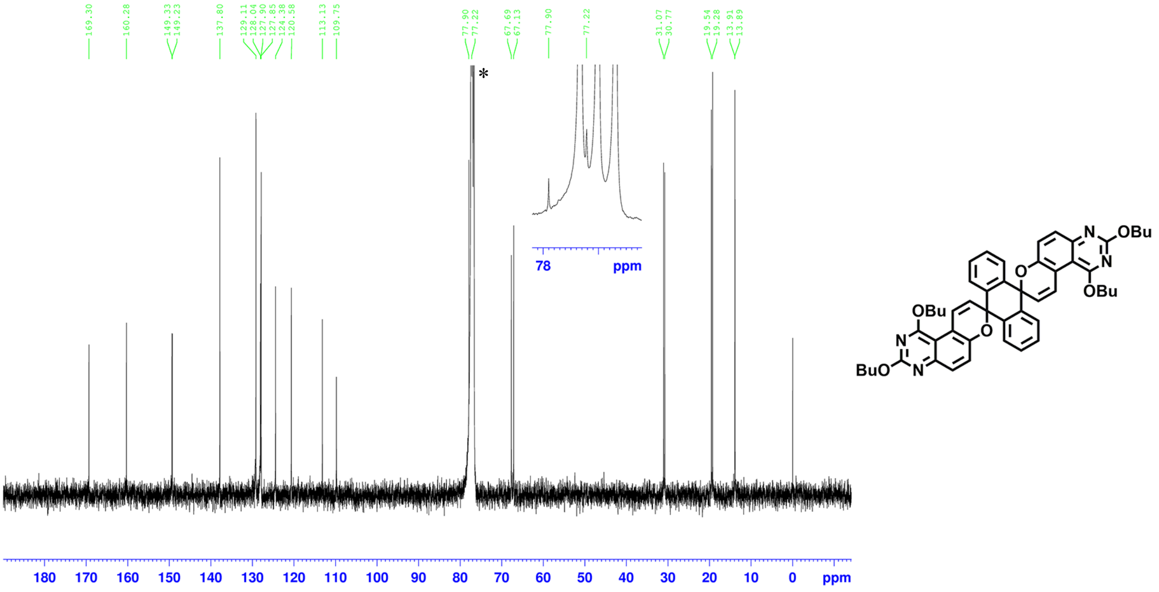

Fig. S8 ^{13}C NMR spectrum of **bis-PQ** in DMSO-d_6 (* solvent peaks).

2. HR-ESI-TOF MS Spectra

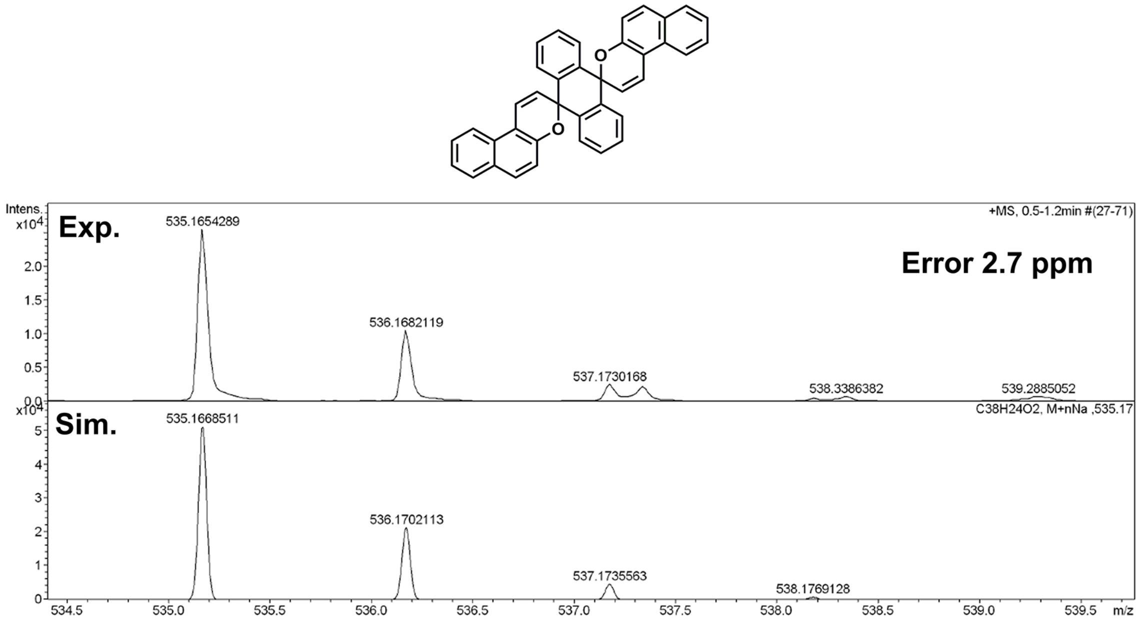

Fig. S9 HR-ESI-TOF MS spectra of **bis-NP**.

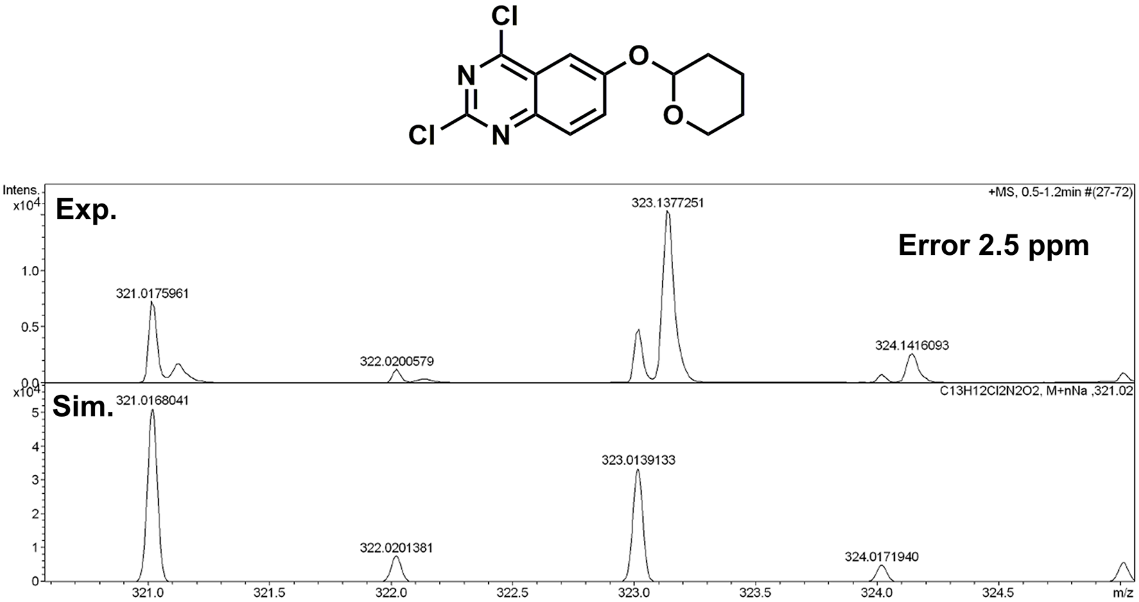

Fig. S10 HR-ESI-TOF MS spectra of 2,4-dichloro-6-((tetrahydro-2*H*-pyran-2-yl)oxy)quinazoline.

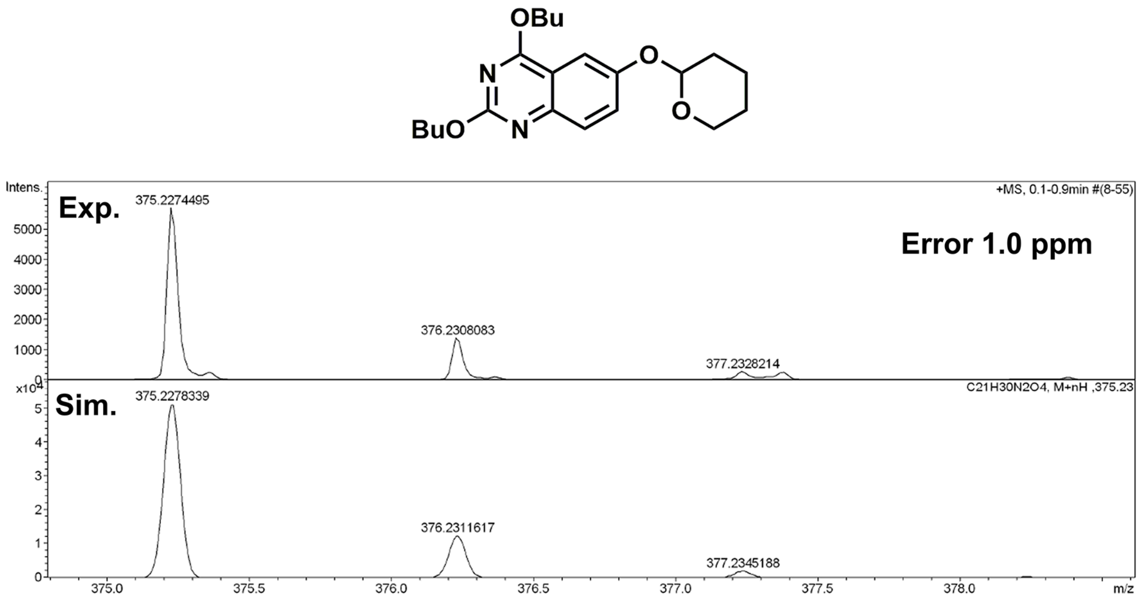

Fig. S11 HR-ESI-TOF MS spectra of 2,4-dibutoxy-6-((tetrahydro-2*H*-pyran-2-yl)oxy)quinazoline.

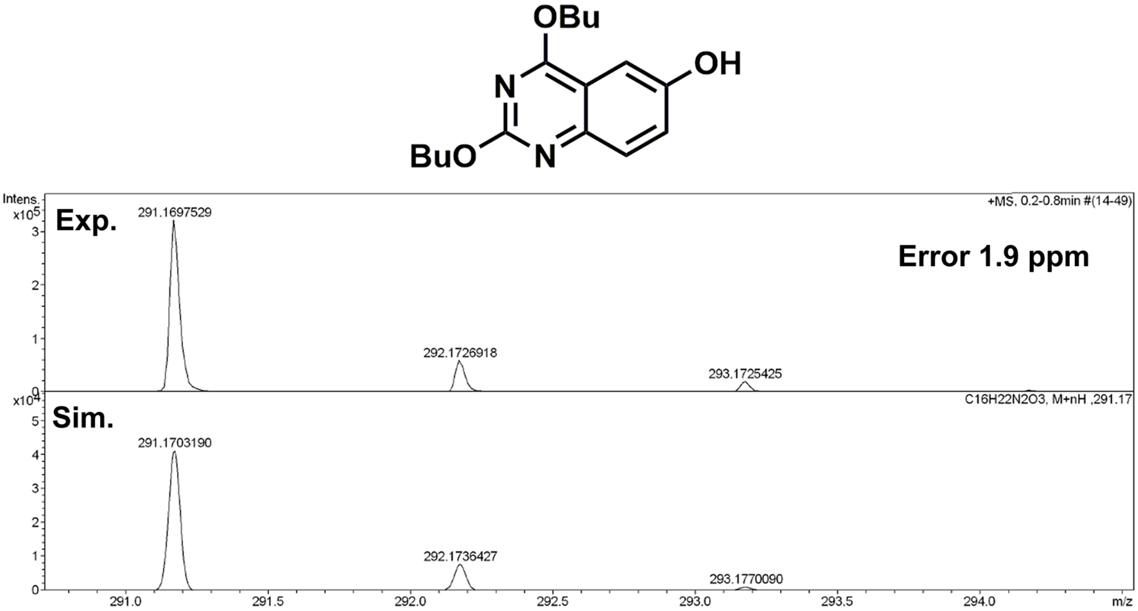

Fig. S12 HR-ESI-TOF MS spectra of 2,4-dibutoxyquinazolin-6-ol.

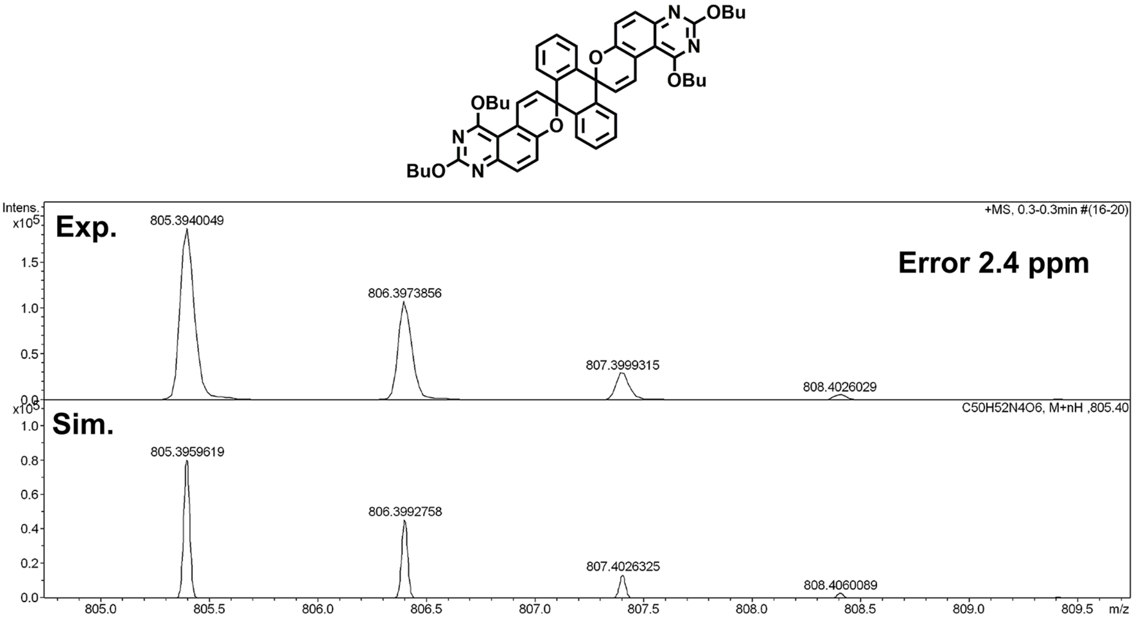

Fig. S13 HR-ESI-TOF MS spectra of **bis-PQ**.

3. HPLC Chromatograms

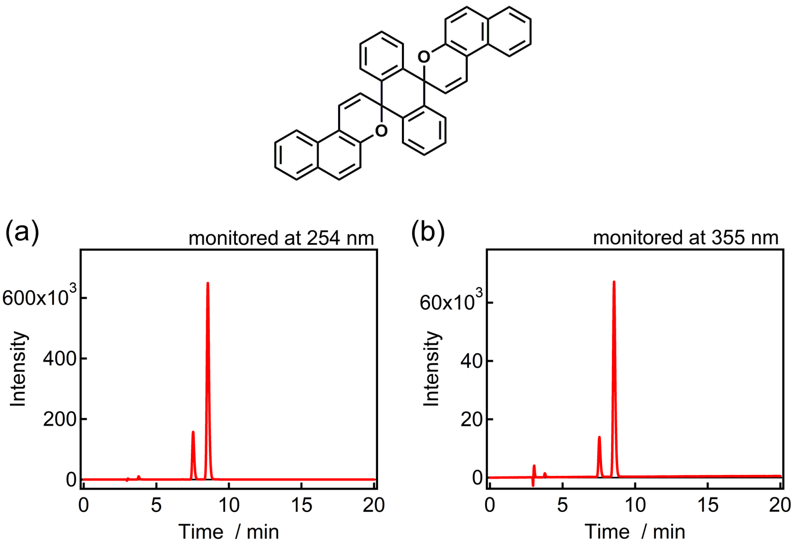

Fig. S14 HPLC chromatograms of **Bis-NP**; 99 % purity (the ratio of the structural isomers = 1:5). HPLC analysis was performed using a reverse phase analytical column (Mightysil RP18, 25cm×4.6mm, 5μm particle) from Kanto Chemical Industries, equipped with a UV detector; the mobile phase was CH_3CN with a flow rate of 1.0 mL/min (detection wavelength; 254 and 355 nm).

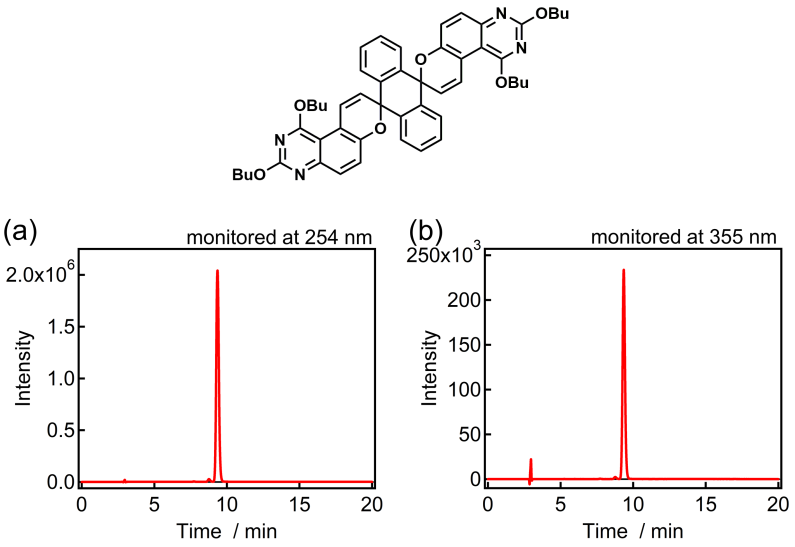

Fig. S15 HPLC chromatograms of **Bis-PQ**; 99 % purity. HPLC analysis was performed using a reverse phase analytical column (Mightysil RP18, 25cm×4.6mm, 5μm particle) from Kanto Chemical Industries, equipped with a UV detector; the mobile phase was CH_3CN:THF = 5:1 with a flow rate of 1.0 mL/min (detection wavelength; 254 and 355 nm).

4. X-ray Crystallographic Analyses

The diffraction data of the single crystals were collected on the Bruker APEX II CCD area detector (Mo Kα, λ = 0.71073 nm). The data refinement was carried out by the Bruker APEXII software package with SHELXT program.[S1] All non-hydrogen atoms were anisotropically refined.

Table S1. Crystallographic Parameters of **bis-NP**

Empirical formula	$C_{38}H_{22.20}O_2$
Formula weight	512.76
Temperature	90(0) K
Wavelength	0.71073 Å
Crystal system	monoclinic
Space group	P 1 21/c 1
Unit cell dimensions	a =7.538(2) Å α = 90°
	b = 9.367(3) Å β = 100.039(4)°
	c = 18.374(5) Å γ = 90°
Volume	1277.5(6) $Å^3$
Z	2
Density (calculated)	1.328 g/m^3
Absorption coefficient	0.081 mm^{-1}
F(000)	532
Theta range for data collection	2.25 to 26.44°
Index ranges	-8<=h<=9, -11<=k<=11, -13<=l<=22
Reflections collected	6578
Independent reflections	2616 [R(int) = 0.0446]
Absorption correction	Empirical
Refinement method	Full-matrix least-squares on F^2
Data / restraints / parameters	2616 / 150 / 60
Goodness-of-fit on F^2	1.035
Final R indices [I>2sigma(I)]	R1 = 0.0740, wR2 = 0.1853
R indices (all data)	R1 = 0.0993, wR2 = 0.2043
Largest diff. peak and hole	0.543 and -0.499 $eÅ^{-3}$

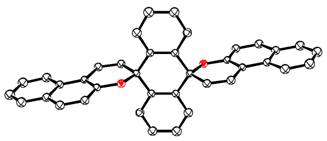

Fig. S16. ORTEP representation of the molecular structure of **bis-NP** with thermal ellipsoids (50 % probability), where oxygen atoms are highlighted in red. The hydrogen atoms are omitted for clarity.

5. Transient UV−Vis Absorption Spectroscopy

One Photon Photochromic Reaction

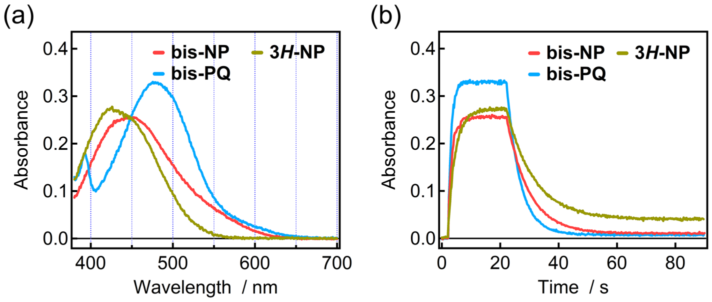

Fig. S17 (a) The transient absorption spectra of **3*H*-NP**, **bis-NP** and **bis-PQ** in toluene (1.8×10^{-5} M) at 298 K upon UV light irradiation (365 nm, 30 mW, for 20 s). (b) Time variations of the absorbance at λ_{max} of **3*H*-NP**, **bis-NP** and **bis-PQ** in toluene under UV light irradiation, and the following thermal back faiding when the irradiation was stopped. The decay curves were fitted by the monoexponential function (eq 1).

$$f_{(t)} = Ae^{-kt} + C \qquad (1)$$

Table S2. Photochromic and Reaction Kinetics Parameters of the TC Form and the Formation Ratios of the TT Form of **bis-NP**, **bis-PQ** and **3*H*-NP**.

	λ_{max} [nm]	A	C	k [s^{-1}]	$\tau_{1/2}$ [s]	TT form [%][a]
bis-NP	447	0.24	1.0×10^{-2}	0.13	5.2	4
bis-PQ	478	0.32	7.5×10^{-3}	0.22	3.1	2
3*H*-NP	425	0.23	4.0×10^{-2}	0.11	6.5	15

(a) The formation ratio of the TT form was defined as C/(C+A) by assuming the molar extinction coefficients of the TC and TT forms are same.

Dependence of Photochromism on Excitation Intensity and Temperature

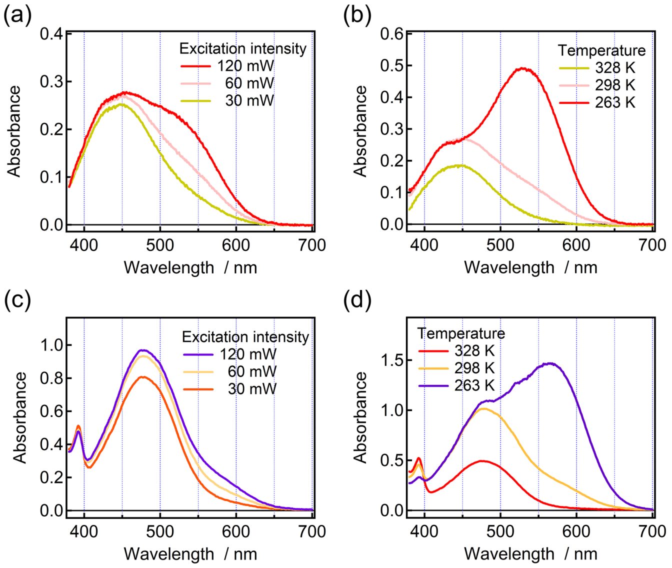

Fig. S18 UV-Vis absorption spectra of **bis-NP** and **bis-PQ** in toluene (1.8×10^{-5} M and 5.0×10^{-5} M, respectively) at the PSS (a, c) under CW UV light irradiation (365 nm, 30–120 mW) at 298 K and (b, d) under CW UV light irradiation (365 nm, 120 mW) at 263, 298 and 328 K.

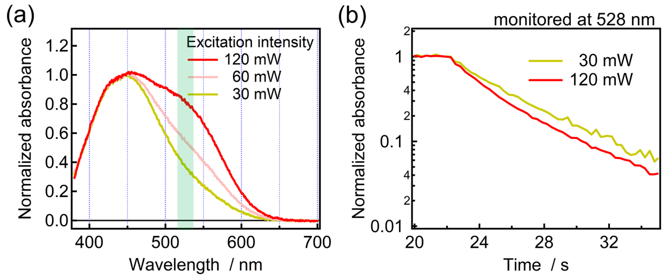

Fig. S19 (a) UV-Vis absorption spectra of **bis-NP** in toluene (1.8×10^{-5} M) at the PSS under CW UV light irradiation (365 nm, 30–120 mW) at 298 K. (b) Time variations of the absorbance at 528 nm of **bis-NP** in toluene (1.8×10^{-5} M) under UV light irradiation (365 nm, 120 mW, for 20 s), and the following thermal back faiding when the irradiation was stopped.

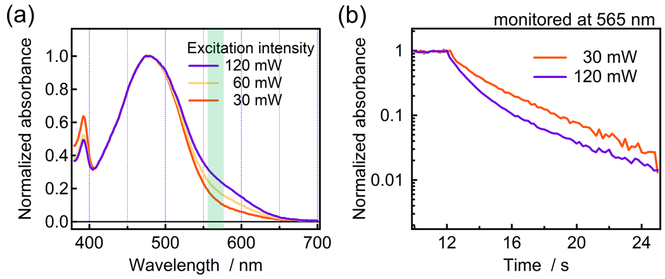

Fig. S20 (a) UV-Vis absorption spectra of **bis-PQ** in toluene (5.0×10^{-5} M) at the PSS under CW UV light irradiation (365 nm, 30–120 mW) at 298 K. (b) Time variations of the absorbance at 565 nm of **bis-PQ** in toluene (5.0×10^{-5} M) under UV light irradiation (365 nm, 120 mW, for 10 s), and the following thermal back faiding when the irradiation was stopped.

Thermal Back Reaction Kinetics of Open-Open Forms

The open-open form of bispyrans is expected to exist as a mixture of TC-TC, TC-TT and TT-TT forms. The formation ratios of the TC and TT forms of **bis-PQ** upon weak UV light irradiation were estimated to be 98% and 2%, respectively (Table S2). The formation ratios of the TC-TC, TC-TT and TT-TT forms of **bis-PQ** can be roughly calculated to be TC-TC: 0.98×0.98×100 = 96.06%, TC-TT: 0.98×0.02×2×100 = 3.90% and TT-TT: 0.02×0.02×100 = 0.04%, respectively, by assuming that: (1) both pyran units in the CC form react independently; (2) the difference in temperature does not affect the production ratios of the TC and TT forms upon UV irradiation and (3) the contributions of TC and TT to the absorption spectrum are equivalent. Therefore, the generation of TT-TT can be neglected. On the other hand, the time profile of the transient absorbance at 610 nm of **bis-PQ** at 263 K can be well fitted by a double exponential function (eq. 2).

$$f_{(t)} = A_1 e^{-k_1 t} + A_2 e^{-k_2 t} \qquad (2)$$

The rate constants, k_1 and k_2, were estimated to be 10 min^{-1} and 1.7 min^{-1}, respectively. This result suggests that the photogenerated open-open form exists as a mixture of the two structural isomers. By the assumption of (3), the formation ratio of the two structural isomers is experimentally defined as A_1:A_2, and was estimated to be 30:70. This experimentally estimated formation ratio of the two structural isomers is not consistent with the theoretically expected formation ratio of TC-TC and TC-TT (=96.06:3.90), indicating that the two decay components for the thermal back reaction of the open-open form of **bis-PQ** can be assigned to the two structural isomers of TC-TC as shown in Scheme S1.

The decay curve of the transient absorbance at 591 nm of **bis-NP** at 263 K can be fitted by a double exponential function. The rate constants of the two decay components were estimated to be 10 min^{-1} and 1.7 min^{-1} and the formation ratio (A_1:A_2) was estimated to be 82:18. This estimated formation ratio of the two decay components for **bis-NP** is largely different from that of **bis-PQ**. The formation ratios of the TC-TC, TC-TT and TT-TT forms of **bis-NP** were roughly calculated to be 92.16 %, 7.68 % and 0.16 %, respectively, in the similar manner with the calculation for **bis-PQ**. In contrast to the formation ratio of TC-TT of **bis-PQ**, the large contribution of the formation of TC-TT of **bis-NP** cannot be ignored because the theoretical ratio of TC-TT (7.68%) is relatively close to the experimentally estimated ratio of one of the decay components (18%). Therefore, it is plausible that TC-TT is generated upon UV light irradiation to **bis-NP** in addition to the structural isomers presented in the above discussion for **bis-PQ** (Scheme 2).

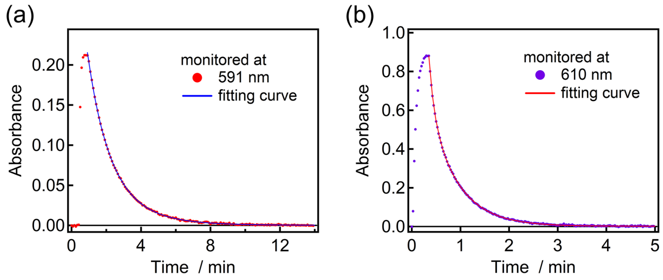

Fig. S21 Time variations of the absorbance of (a) **bis-NP** at 591 nm and (b) **bis-PQ** at 610 nm in toluene (1.8×10^{-5} M and 5.0×10^{-5} M, respectively) at 263 K under UV light irradiation, and the following thermal back faiding when the irradiation was stopped. The decay curves were fitted by the double exponential function (eq. 2).

Table S3. Reaction Kinetics Parameters for the Thermal Back Reaction of the Open-Open form of **bis-NP** and **bis-PQ** in Toluene (1.8×10^{-5} M and 5.0×10^{-5} M, respectively) at 263 K.

	A_1	k_1	A_2	k_2
bis-NP	0.18	0.79	0.039	0.42
bis-PQ	0.26	10	0.62	1.7

The reaction kinetic parameters were estimated from the fitting curve of the time variation of the absorbance by the double exponential function (eq. 2).

6. Plausible Photochromic Reaction

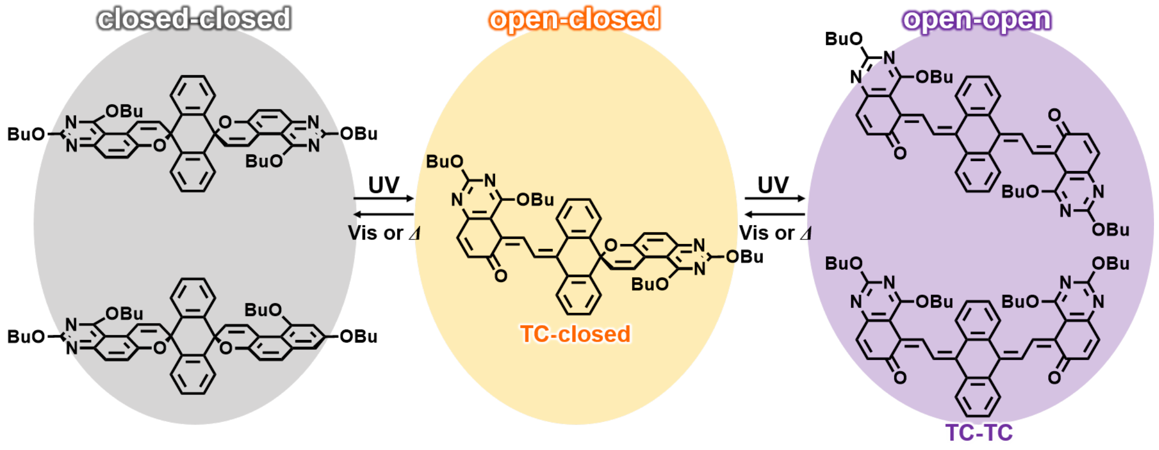

Scheme S1. The plausible stepwise two-photon photochromic reaction scheme of **bis-PQ**.

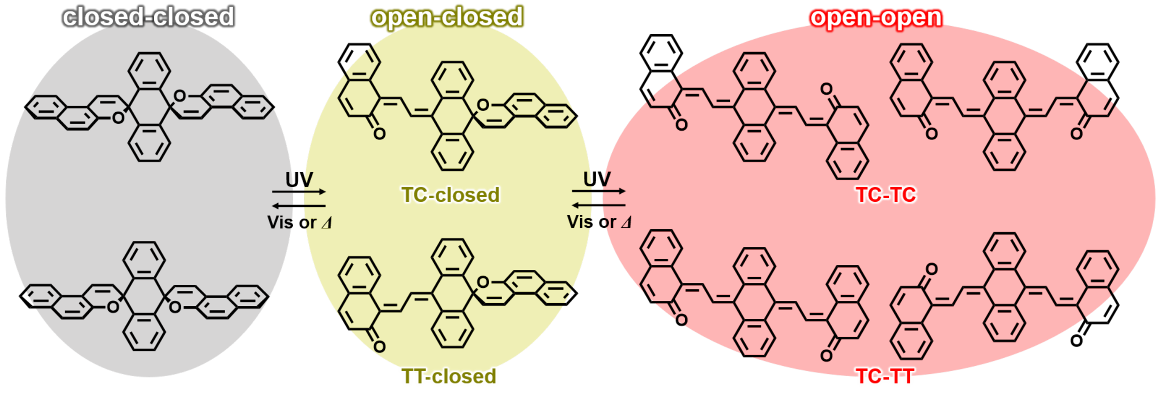

Scheme S2. The plausible stepwise two-photon photochromic reaction scheme of **bis-NP**.

7. References

S1. (a) Sheldrick GM. SHELXS-97 and SHELXL-97; University of Gottingen, Germany, 1997.

(b) Sheldrick GM. SADABS; University of Gottingen, Germany, 1996.